Laukkanen, Olli Ville; Winter, H. Henning

The dynamic fragility and apparent activation energy of bitumens as expressed by a modified Kaelble equation

Published in:
Journal of Non-Crystalline Solids

DOI:
10.1016/j.jnoncrysol.2018.07.036

Published: 01/11/2018

Document Version
Peer-reviewed accepted author manuscript, also known as Final accepted manuscript or Post-print

The dynamic fragility and apparent activation energy of bitumens as expressed by a modified Kaelble equation

Olli-Ville Laukkanen[1,2] and H. Henning Winter[1]

[1] Department of Polymer Science and Engineering & Department of Chemical Engineering, University of Massachusetts, Amherst, MA 01003, United States

[2] Department of Chemical and Metallurgical Engineering, School of Chemical Engineering, Aalto University, P.O. Box 16100, 00076 Aalto, Finland

Abstract The temperature dependence of the dynamics of glass-forming liquids can be characterized by the dynamic fragility (m) and apparent activation energy (E_a) at the glass transition temperature T_g. In this study, we derive analytical expressions that allow the calculation of these parameters from a modified Kaelble equation which divides the temperature dependence into two regimes above and below a characteristic temperature T_d. Special emphasis is given to the analysis of the T_d parameter that can be considered as the rheological glass transition temperature. Rheological characterization is performed on twenty-seven bitumens originating from various crude oil sources and refining processes. Their dynamic fragilities and apparent activation energies are calculated at the calorimetric T_g and at T_d. Bitumen can be classified as a strong glass-forming liquid, dynamic fragilities varying in the range of $m(T_g)$ = 26 … 52 for the individual bitumen samples. The results indicate that $m(T_g)$ and $E_a(T_g)$ are linearly correlated with T_g, and these T_g-dependences are unusually strong in comparison to other classes of glass-forming liquids. However, dynamic fragilities and apparent activation energies evaluated at T_d are nearly independent of the type of bitumen and show only a weak dependence on T_d.

Keywords Dynamic fragility, Apparent activation energy, Modified Kaelble equation, Rheology, Bitumen

1. Introduction

Petroleum bitumen, a residue of crude oil distillation, is widely used as a binder in asphalt pavements [1]. It is an extremely complex mixture of different molecular constituents that vary in chemical composition and molecular weight [2,3]. Although mainly composed of low-molecular-weight hydrocarbons, bitumen also contains significant amounts of heteroatoms such as sulfur, nitrogen and oxygen, as well as traces of metals like vanadium and nickel [4]. The physical properties of bitumen are largely governed by complex molecular interactions including dispersive, polar, hydrogen bonding and π-π interactions [5]. In particular, the rheological properties of bitumen have been shown to be heavily influenced by aromatic interactions [5–7] and by the content of carbonyl and sulfoxide functional groups [8]. Moreover, the chemical composition and therefore the physical properties of bitumen depend on the crude oil source and on the refining processes employed in its production [9].

Bitumen is known to be a complex glass-forming liquid [10–12] with a glass transition at around -20 °C, the exact glass transition temperature being dependent mainly on the crude oil

it originates from [13–17]. Due to its extreme chemical and structural complexity, bitumen exhibits unusual rheological characteristics as compared to most other glass-forming liquids. Most importantly, a significant broadening of the viscoelastic glass transition is observed [11,12]. However, although numerous studies have been performed to study the rheological properties of bitumen at low temperatures, no one has yet specifically studied the temperature dependence of these properties at the glass transition.

The temperature dependence of the viscoelastic properties of glass-forming liquids is commonly described by two coupled parameters: dynamic fragility, m, and apparent activation energy, E_a, at T_g [18]. The dynamic fragility, also known as the steepness index [19], characterizes the rapidity with which a liquid's dynamic properties change as the glass transition temperature is approached and is quantified as [20]:

$$m(T_g) = \left[\frac{\mathrm{d}\log a_T}{\mathrm{d}(T_g/T)}\right]_{T=T_g} \tag{1}$$

where a_T is the time-temperature shift factor. This parameter measures the deviation from the Arrhenius temperature dependence in the vicinity of T_g [21]. When $m(T_g)$ is high, the material exhibits highly non-Arrhenius temperature dependence and we refer to it as a fragile liquid. On the contrary, when $m(T_g)$ is low, the material shows (nearly) Arrhenius-type temperature dependence and it is said to be a strong liquid. The apparent activation energy at T_g can be readily calculated from the dynamic fragility:

$$E_a(T_g) = \ln(10)\, R T_g m(T_g) \tag{2}$$

where R is the universal gas constant, 8.314 J mol^{-1} K^{-1}. Consequently, the dynamic fragility can be understood as a T_g-normalized activation energy.

Traditionally, the temperature dependence of relaxation patterns in the vicinity of T_g is modelled with the Vogel–Fulcher–Tammann (VFT) [22–24] or Williams–Landel–Ferry (WLF) [25] equation. In this case, dynamic fragility and apparent activation energy can be rewritten in terms of VFT and WLF parameters [18]. For the WLF equation:

$$\log a_T = \frac{-c_1(T - T_{ref})}{c_2 + T - T_{ref}} \tag{3}$$

$$m(T_g) = \frac{c_1^g T_g}{c_2^g} \tag{4}$$

$$E_a(T_g) = \ln(10)\, R \frac{c_1^g T_g^2}{c_2^g} \tag{5}$$

where c_1 and c_2 are the WLF parameters at an arbitrary reference temperature T_{ref}, and c_1^g and c_2^g represent the values of c_1 and c_2 when $T_{ref} = T_g$.

However, as reviewed by McKenna and Zhao [26], recent theoretical [27–34] and experimental [35–43] studies suggest that time scales actually do not diverge at temperatures above zero Kelvin, i.e. the temperature dependence of viscoelastic properties deviate from the VFT/WLF behavior below T_g. In fact, deviations from the VFT/WLF behavior are often

observed even slightly above T_g (typically around T_g+10 K), see e.g. Refs. [11,44–46]. Consequently, $m(T_g)$ and $E_a(T_g)$ values calculated from the VFT/WLF fits (Eqs. 4 and 5) cannot always be considered reliable. Several modifications have been proposed to the traditional WLF equation to describe the temperature dependence of relaxation processes both above and below T_g by a single relation [47–54]. Most notably, Rowe and Sharrock [55] have proposed the following equation that is commonly known as the modified Kaelble equation:

$$\log a_T = \frac{-c_1(T - T_d)}{c_2 + |T - T_d|} \tag{6}$$

where T_d defines the temperature at which the curvature of the S-shaped log a_T versus T curve changes from positive to negative. It should be noted that this equation is a modification of the shift factor model initially proposed by Kaelble [54]. The general shape of the modified Kaelble equation is illustrated in Fig. 1. Above T_d, Eqs. (3) and (6) are identical when $T_{ref} = T_d$. Below T_g, Eq. (3) predicts too rapid a rise in log a_T culminating in a predicted infinite positive value when $T = T_{ref}$-c_2. Conversely, Eq. (6) predicts non-diverging time scales below T_g in a fashion consistent with experimental data. However, it is not straightforward to fit Eq. (6) to data since the form of this equation inherently assumes that the defining temperature and the reference temperature are the same, $T_{ref} = T_d$. This difficulty can be overcome by the addition of a constant term that separates T_d from T_{ref} [55]:

$$\log a_T = -c_1\left(\frac{T - T_d}{c_2 + |T - T_d|} - \frac{T_{ref} - T_d}{c_2 + |T_{ref} - T_d|}\right) \tag{7}$$

It can be easily shown that Eqs. (6) and (7) are mathematically identical.

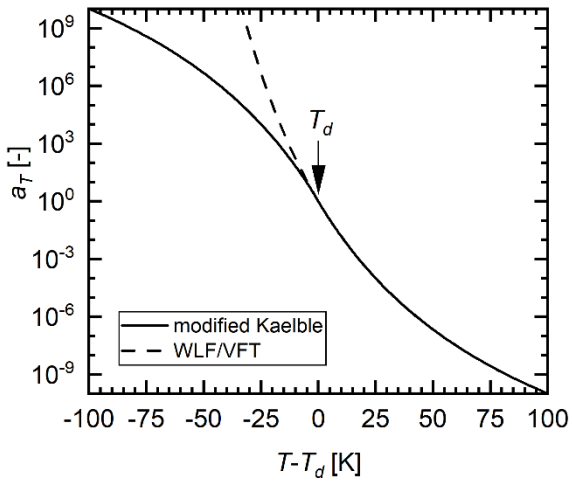

Fig. 1 Schematic representation of the modified Kaelble equation. A curve corresponding to the traditional WLF/VFT equation is shown for comparison purposes.

It has been shown that the modified Kaelble equation accurately captures the temperature dependence of various viscoelastic materials both above and below T_g. These materials include different types of asphalt binders and mixtures [11,55–58], as well as various polymers (e.g. polymethylmethacrylate [54], polystyrene [54,55], polyisoprene [59] and polyurethane [59]) and commercial damping materials (e.g. EAR C-1002 [59] and Hunston [59]). Moreover, we

expect that the modified Kaelble equation can accurately describe the temperature dependence of many other viscoelastic materials too, although this needs to be confirmed by further studies.

In this paper, we analytically derive equations that allow the calculation of m and E_a from the fits of the modified Kaelble equation. These equations are used to calculate the m and E_a values of a wide variety of bitumens at T_g and T_d. Furthermore, the T_g-dependences of these parameters are examined and compared with other types of glass-forming liquids.

2. Theory

2.1. Analytical derivation of $m(T_g)$ and $E_a(T_g)$ from the modified Kaelble equation

In this section, we derive analytical equations for calculating $m(T_g)$ and $E_a(T_g)$ using parameter values obtained from the fit of the modified Kaelble equation, Eq. (7). Upon differentiation with respect to T_g/T, the second term of Eq. (7) becomes zero (derivative of a constant). Thus, we can start the derivation of the dynamic fragility from the modified Kaelble equation by considering the form of Eq. (6). When $T \leq T_d$, this equation can be written as follows:

$$\log a_T = \frac{-c_1(T - T_d)}{c_2 - T + T_d} = \frac{-c_1 T_g \left(\frac{T}{T_g}\right) + c_1 T_d}{c_2 - T_g \left(\frac{T}{T_g}\right) + T_d} \tag{8}$$

By substituting

$$u = \frac{T_g}{T} \Leftrightarrow u^{-1} = \frac{T}{T_g} \tag{9}$$

into Eq. (8), the following equation is obtained:

$$\log a_T = \frac{-c_1 T_g u^{-1} + c_1 T_d}{c_2 - T_g u^{-1} + T_d} \tag{10}$$

As described by Eq. (1), the dynamic fragility is defined as the derivative of the time-temperature shift factor with respect to T_g-normalized inverse temperature. Considering the substitution of Eq. (9) and the expression of Eq. (10), Eq. (1) can be rewritten as:

$$m(T_g) = \left[\frac{\mathrm{d}\log a_T}{\mathrm{d}\left(\frac{T_g}{T}\right)}\right]_{T=T_g} = \left[\frac{\mathrm{d}\log a_T}{\mathrm{d}u}\right]_{T=T_g} = \left[\frac{\mathrm{d}\left(\frac{-c_1 T_g u^{-1} + c_1 T_d}{c_2 - T_g u^{-1} + T_d}\right)}{\mathrm{d}u}\right]_{T=T_g} \tag{11}$$

Further, after simplification, the following expression is found for the dynamic fragility:

$$m(T_g) = \left[\frac{c_1 c_2 T_g u^{-2}}{\left(c_2 - T_g u^{-1} + T_d\right)^2}\right]_{T=T_g} \tag{12}$$

After the back-substitution of Eq. (9) into Eq. (12) and simplification, the following expression is obtained for the dynamic fragility:

$$m(T_g) = \left[\frac{c_1 c_2 \frac{T^2}{T_g}}{(c_2 - T + T_d)^2}\right]_{T=T_g} \tag{13}$$

Finally, the dynamic fragility is determined at $T = T_g$:

$$m(T_g) = \frac{c_1^g c_2^g T_g}{(c_2^g - T_g + T_d)^2} \tag{14}$$

Correspondingly, when $T \geq T_d$, Eq. (1) can be written as follows:

$$\log a_T = \frac{-c_1(T - T_d)}{c_2 + T - T_d} \tag{15}$$

In this case the derivation of $m(T_g)$ follows the same steps outlined in Eqs. (8)-(14), only some sign changes are required. Finally, an equation equivalent to Eq. (14) is obtained:

$$m(T_g) = \left[\frac{c_1 c_2 \frac{T^2}{T_g}}{(c_2 + T - T_d)^2}\right]_{T=T_g} = \frac{c_1^g c_2^g T_g}{(c_2^g + T_g - T_d)^2} \tag{16}$$

Finally, it is noted that Eqs. (14) and (16) can be combined into a single equation that is valid at all temperatures, i.e. both when $T_g \leq T_d$ and when $T_g > T_d$:

$$m(T_g) = \frac{c_1^g c_2^g T_g}{\left(c_2^g + |T_d - T_g|\right)^2} \tag{17}$$

Correspondingly, an analytical solution for the apparent activation energy at T_g is obtained by substituting Eq. (17) into Eq. (2):

$$E_a(T_g) = \ln(10)\, R T_g m(T_g) = \frac{\ln(10)\, c_1^g c_2^g R T_g^2}{\left(c_2^g + |T_d - T_g|\right)^2} \tag{18}$$

2.2. Dynamic fragility and apparent activation energy at T_d

As noted earlier, the T_d parameter of the modified Kaelble equation defines the temperature at which an inflection point appears in the log a_T versus T curve (Fig. 1). Similarly, there is an inflection point at T_d when shift factors are plotted against inverse temperature (Fig. 2). This means that in both of these plotting methods, the slope of the shift factor curve is at its largest at T_d. To highlight this characteristic, the derivative of the modified Kaelble equation with respect to inverse temperature is plotted in Fig. 2. The analytical form of this derivative has been solved above (Eqs. (13) and (16)) and can be written as follows using the parameters of the modified Kaelble equation:

$$\frac{\mathrm{d}\log a_T}{\mathrm{d}\left(\frac{T_g}{T}\right)} = \frac{c_1^g c_2^g T^2}{\left(c_2^g + |T_d - T|\right)^2 T_g}\ , \text{ where } \log a_T = \frac{-c_1(T - T_d)}{c_2 + |T - T_d|} \tag{19}$$

Obviously, this derivative attains its highest value at the inflection point $T = T_d$. In practical terms, T_d corresponds to the temperature at which the temperature dependence of viscoelastic properties is largest. Consequently, this temperature can be considered as the rheological glass transition temperature [60,61]. It is worth noting that, as far as the authors know, T_d provides the only unambiguous definition of the rheological glass transition temperature. By this we mean that T_d is completely independent of experimental parameters such as measurement frequency and heating/cooling rate. However, the theoretical basis of T_d is still unclear and beyond the scope of this paper. Following Eq. (19), the dynamic fragility and apparent activation energy at T_d can be defined as follows using the modified Kaelble parameters:

$$m(T_d) = \left[\frac{\mathrm{d}\log a_T}{\mathrm{d}\left(\frac{T_g}{T}\right)}\right]_{T=T_d} = \frac{c_1^g {T_d}^2}{c_2^g T_g}\ , \text{ where } \log a_T = \frac{-c_1(T - T_d)}{c_2 + |T - T_d|} \tag{20}$$

$$E_a(T_d) = \ln(10)\, R T_g m(T_d) = \ln(10)\, R \frac{c_1^g {T_d}^2}{c_2^g} \tag{21}$$

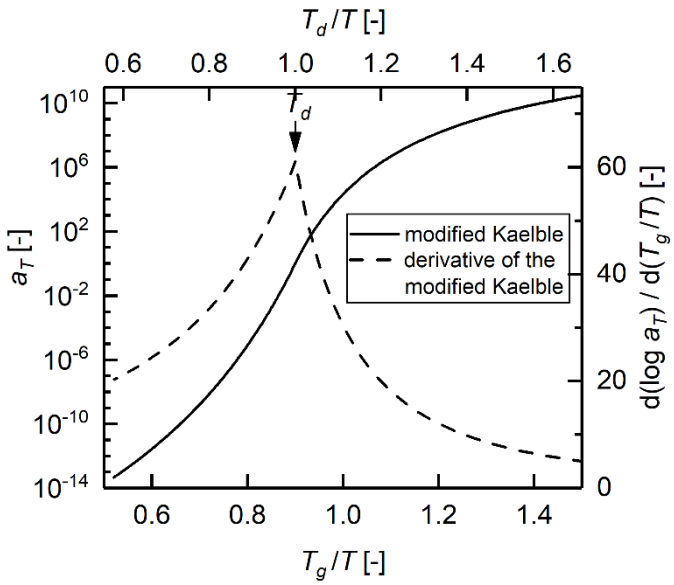

Fig. 2 Schematic representation of the modified Kaelble equation and its derivative (Eq. (19)) in the Angell plot. In this example, $T_g / T_d = 0.9$.

3. Materials and methods

In this study, we investigated twenty-seven bitumen samples originating from various crude oil sources and refining processes. Details of these samples are given in our previous publications [6,62] and are not repeated here for brevity. It is worth emphasizing that this

sample set covers exceptionally wide variation in physical and chemical properties, some of these bitumens not even being suitable for industrial use in asphalt paving applications.

Rheological properties of the bitumen samples were measured on stress-controlled Malvern Kinexus Pro and Paar Physica MCR 500 rheometers. Both of these rheometers were equipped with a Peltier plate and active hood to provide a mostly accurate and gradient-free control of the specimen temperature. Frequency sweep experiments (ω = 0.0628 – 62.8 rad/s) were performed in the linear viscoelastic regime at temperatures ranging from -40 to 90 °C in 10 K intervals. Parallel plate geometries with 4-, 8- and 25-mm diameters were used at different temperature ranges in order to minimize instrument compliance errors [63], and the data measured at the lowest temperatures using the 4-mm parallel plate geometry were corrected for minor compliance effects as described previously [64,65]. It needs to be emphasized that the frequency sweep data were measured in, or at least very close to, the metastable equilibrium state of the bitumen samples. To confirm this, cyclic frequency sweep (CFS) experiments were performed to evaluate the time dependence of rheological properties at various temperatures in the vicinity of T_g. The experimental details and partial results have been reported in our previous publication [11] and will be discussed further in our forthcoming paper [66]. As an example, Fig. 3 plots aging time shift factors a_{te} – obtained by means of time-aging time superposition – as a function of aging time t_e for bitumen sample B-18. Note that only horizontal shifts are necessary to obtain good superposition in this case (see Ref. [66] for details). The aging time shift factors are observed to be relatively small at all the temperatures studied, demonstrating that only minor physical aging takes place in this sample. It can therefore be concluded that physical aging has a negligible effect on the time-temperature shift factors a_T analyzed in the following section of this paper. Further details of the specimen preparation and measurement protocols can be found elsewhere [6,62].

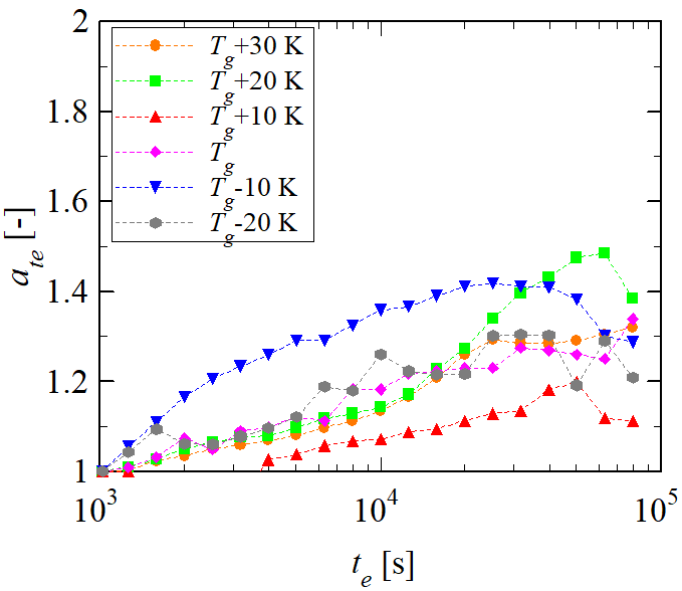

Fig. 3 The aging time shift factors of bitumen sample B-18 (T_g = -20 °C) plotted as a function of aging time at various aging temperatures. The aging time shift factors were obtained by means of the time-aging time superposition of cyclic frequency sweep (CFS) data (see Ref. [66] for more details).

Glass transition temperatures were measured by differential scanning calorimetry (DSC), using a Mettler Toledo DSC1 differential scanning calorimeter. The samples were subjected to a cooling scan from 140 to -60 °C at 10 K/min, followed by a heating scan in the same temperature range and at the same scan rate. T_g was taken as the midpoint of the glass transition region upon heating.

4. Results and discussion

An example of the determination of time-temperature shift factors a_T is given in Figs. 4(a)-(c). Frequency sweep curves measured at different temperatures are shifted horizontally to construct master curves at a selected reference temperature. The validity of the time-temperature superposition (TTS) principle is confirmed by the smooth shapes of the loss tangent master curve (Fig. 4(b)) and of the Booij-Palmen plot (Fig. 4(d)) [67]. However, it should be noted that thermorheological simplicity is not a universal property of glass-forming substances. Especially in the case of glassy polymers, the breakdown of the time-temperature superposition principle is often observed as reported by Ngai and Plazek [68], among others. In these cases, obviously, time-temperature shift factors a_T cannot be used to determine the dynamic fragility and apparent activation energy. Fig. 4(c) shows the excellent fit of the modified Kaelble model, Eq. (7), to the empirical shift factors. Similar fits were obtained for all the bitumen samples; the fitted model parameters are summarized in Table 1. This table also includes the dynamic fragility and apparent activation energy values calculated at the calorimetric T_g (Eqs. (17) and (18)) and at T_d (Eqs. (20) and (21)). As noted in Section 2.2., the maximum values for m and E_a are obtained at T_d (corresponding to the steepest slope in the shift factor curve when plotted as a function of T or T_g/T).

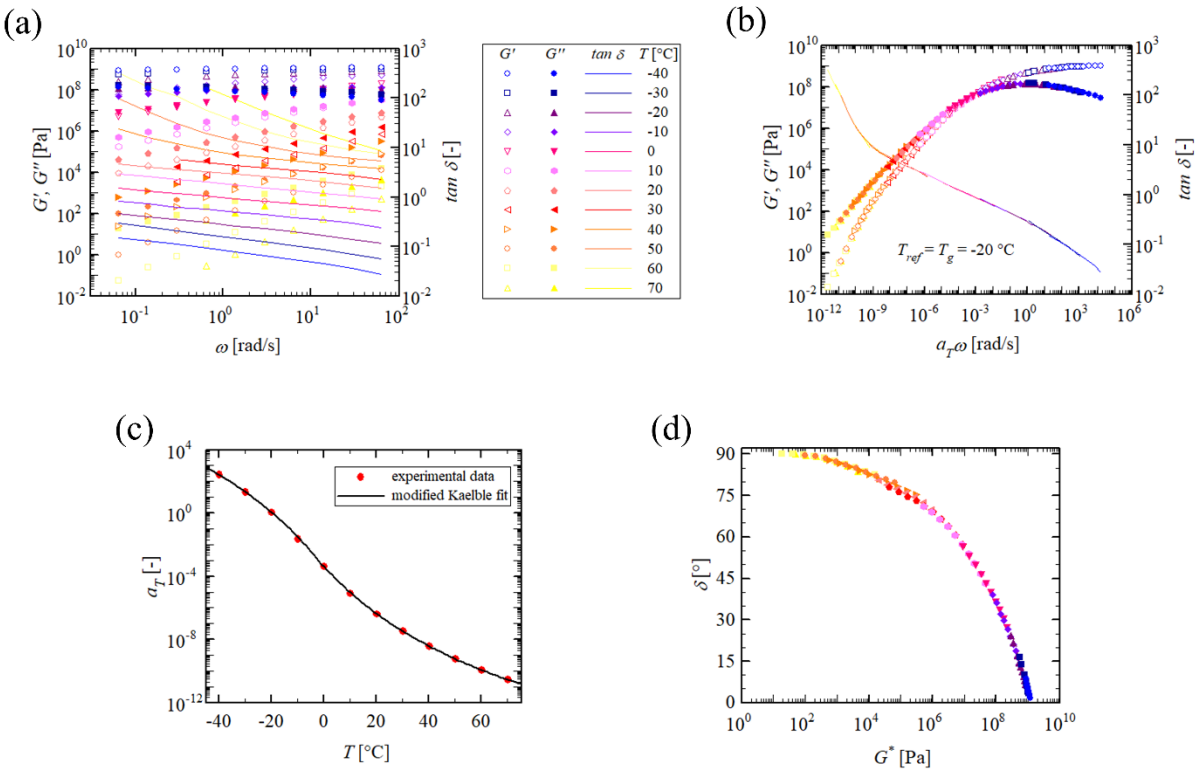

Fig. 4 Example of the determination of time-temperature shift factors a_T from the frequency sweep data measured at different temperatures. (a) Data from the frequency sweep experiments. (b) Master curves constructed by horizontally shifting the frequency sweep data according to the TTS principle. (c) Shift factors obtained from the construction of master curves and the fit of the modified Kaelble equation to this data. (d) The thermorheological simplicity of the investigated material is confirmed by the good superposition of the frequency sweep data in the Booij-Palmen plot.

In Table 1, $m(T_g)$ values are observed to vary quite significantly between different bitumen samples. The range of these parameter values is $m(T_g) = 26 \ldots 52$, the average value being $m(T_g) \approx 37$. These values are relatively small compared to many other glass-forming liquids, indicating that bitumen can be considered as a strong glass-forming liquid. In other words, only small deviations from the Arrhenius-type temperature dependence are observed in the vicinity of the glass transition. Correspondingly, the $E_a(T_g)$ values vary in the range of 115 to 271 kJ/mol, the average value being $E_a(T_g) \approx 181$ kJ/mol.

Table 1 Parameter values obtained from the fits of the modified Kaelble equation to the experimental shift factor data. The quality of the fit is expressed by the normalized root-mean-square error (NRMSE). In addition, the table shows dynamic fragility and apparent activation energy values evaluated at T_g and at T_d. Standard deviations (SD) were estimated from three independent replicate measurements (note that repeatability data was not available for T_g). The sample codes (B-1 to B-27) are the same as used in our previous publications [6,62].

Sample	c_1^g [-]	c_2^g [K]	$T_{ref} = T_g$ [K]	T_d [K]	NRMSE [%]	$m(T_g)$ [-] Eq. (17)	$E_a(T_g)$ [kJ/mol] Eq. (18)	$m(T_d)$ [-] Eq. (20)	$E_a(T_d)$ [kJ/mol] Eq. (21)
SD	*0.36*	*3.9*	*N/A*	*0.35*	-	*0.42*	*2.0*	*1.5*	*7.4*
B-1	27.0	139.0	263	270.1	0.66	46	231	54	271
B-2	19.8	92.9	275	281.3	0.61	51	267	61	323
B-3	19.3	91.2	269	273.0	0.83	52	271	59	302
B-4	26.3	130.3	259	268.6	0.61	45	223	56	279
B-5	18.5	87.8	263	274.5	0.59	44	221	60	304
B-6	18.3	86.8	264	273.5	0.60	45	225	60	302
B-7	19.2	99.8	251	270.5	0.35	34	162	56	269
B-8	17.4	79.5	259	272.3	0.56	42	207	63	311
B-9	20.1	102.3	250	271.1	0.25	34	162	58	276
B-10	22.6	122.0	246	270.9	0.94	31	147	55	260
B-11	18.4	92.8	255	269.9	0.43	38	184	57	277
B-12	19.2	90.0	252	271.4	0.50	36	176	62	301
B-13	23.5	117.9	248	267.9	0.62	36	171	58	274
B-14	19.6	95.9	250	268.9	0.81	36	170	59	283
B-15	17.2	78.7	251	270.9	0.74	35	167	64	307
B-16	18.5	89.0	251	270.1	0.47	36	171	60	290
B-17	20.7	109.0	246	268.2	0.40	32	153	55	262
B-18	17.2	86.2	253	268.8	0.29	36	176	57	276
B-19	21.4	105.2	247	270.3	0.72	34	159	60	285
B-20	17.8	83.4	253	268.7	0.61	38	185	61	295
B-21	31.9	173.6	249	266.0	0.48	38	181	52	249
B-22	18.3	94.3	249	267.7	0.30	34	161	56	266
B-23	20.4	111.9	249	267.0	0.63	33	159	52	249
B-24	17.9	91.2	246	267.3	0.73	32	148	57	268
B-25	16.5	88.6	247	265.4	0.34	32	150	53	251
B-26	21.9	130.0	236	267.5	0.59	26	115	51	231
B-27	17.8	95.6	242	265.9	0.53	29	133	54	252

Variations in the temperature dependences of different bitumen samples are further illustrated in Fig. 5 where the shift factor data is plotted against T_g/T. This type of plot is commonly referred as the Angell plot [69], although the Tg-normalization of the temperature axis was first introduced in the works of Oldekop [70] and Laughlin and Uhlmann [71]. Quite surprisingly, only minor differences in the shapes of the curves are apparent. In the close vicinity of the glass transition ($T_g/T \approx 1$), however, larger variations in the slopes of the curves become visible. This observation is consistent with the relatively large variation of $m(T_g)$ values reported in Table 1. At this point, it is not completely clear why significant differences in the temperature dependences appear only very close to the glass transition.

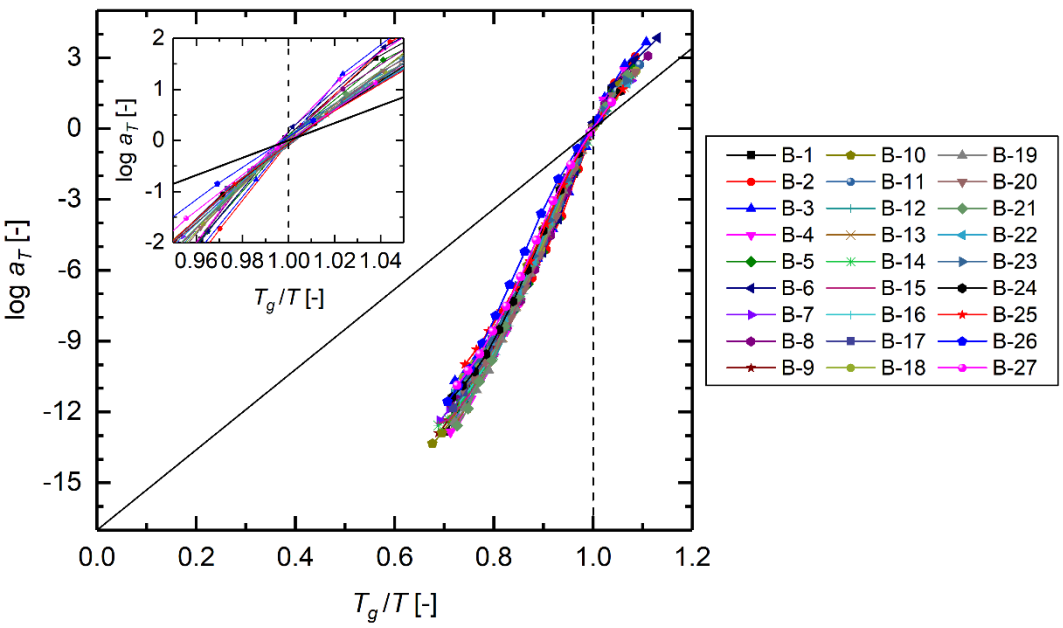

Fig. 5 Angell plot of the investigated bitumen samples. The inset shows a magnification of the plot in the vicinity of T_g (i.e. $T_g/T \approx 1$). The solid line corresponds to the Arrhenius temperature dependence (m = 17) of a strong glass-forming liquid.

Qin and McKenna [18] have suggested that different categories of glass-forming liquids exhibit different behaviors in terms of the T_g-dependence of $m(T_g)$ and $E_a(T_g)$. Fig. 6 shows an evaluation of these dependences in the case of our bitumen samples. Strong positive linear correlations are found both between $m(T_g)$ and T_g, as well as between $E_a(T_g)$ and T_g. However, it must be noted that the investigated bitumen samples exhibited only a narrow range of glass transition temperatures. Since the dynamic fragility is effectively a T_g-normalized activation energy (Eq. (2)), the almost identical T_g-dependences of $m(T_g)$ and $E_a(T_g)$ are expected in this case.

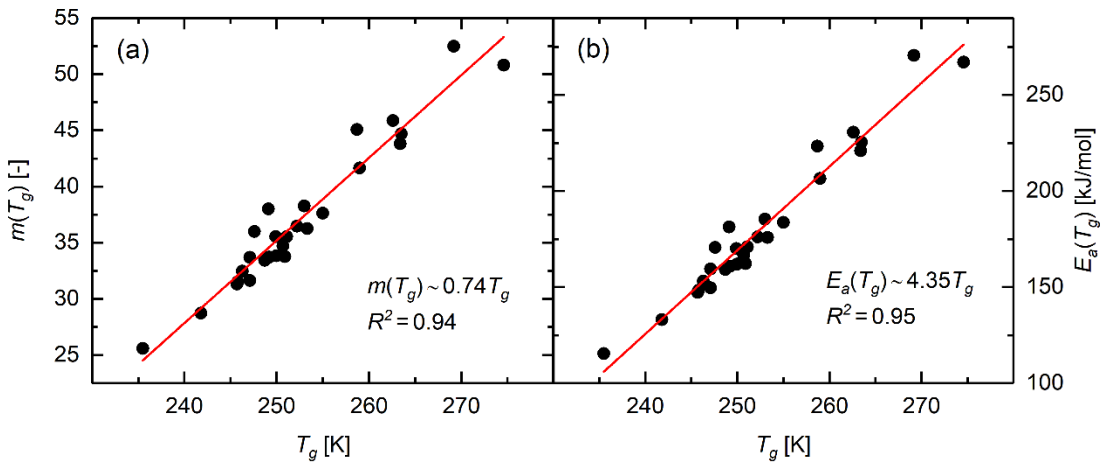

Fig. 6 T_g-dependences of (a) dynamic fragility $m(T_g)$ and (b) apparent activation energy $E_a(T_g)$ in the investigated bitumen samples.

Master plots comparing the T_g-dependences of $m(T_g)$ and $E_a(T_g)$ in different classes of glass-forming liquids are presented in Figs. 7(a) and 7(b), respectively. In addition to the bitumen data of Figs. 6(a) and 6(b), these plots include data for various polymers, small-molecule organics, hydrogen-bonding organics, inorganics, ionic and metallic glass formers, as well as for ionic liquids and ambers. The strengths of the T_g-dependences in the different types of glass-forming liquids are estimated by calculating the slopes of linear regression lines. As suggested by Qin and McKenna [18] and as can be seen from Table 2, different glass formers show largely different T_g-dependences of $m(T_g)$ and $E_a(T_g)$. Most notably, the T_g-dependences of both of these parameters are observed to be stronger in bitumen ($m(T_g) \sim 0.74T_g$ and $E_a(T_g) \sim 4.35T_g$) than in any other type of glass-forming liquids. It is not clear at this time, however, what is the chemical or structural origin of these exceptionally large T_g-dependences. In particular, more complete understanding of bitumen chemistry would be required to make such judgments.

(a)

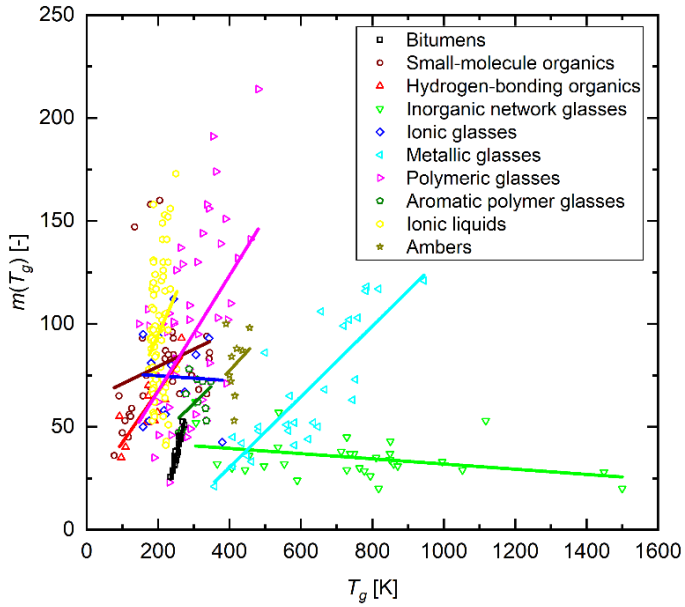

(b)

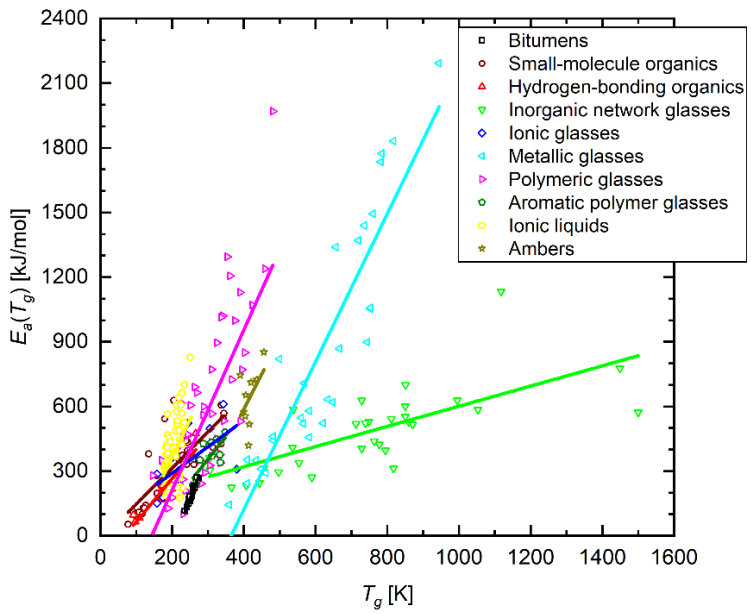

Fig. 7 T_g-dependences of (a) dynamic fragility $m(T_g)$ and (b) apparent activation energy $E_a(T_g)$ in various classes of glass-forming liquids. The solid lines represent linear fits to each individual category of glass-forming liquids. The data has been retrieved from the works of Qin and McKenna [18], Tao et al. [72] and Zhao and McKenna [73]. References to the original data are summarized in the following (see Refs. [18,72,73] for the full details): small-molecule organics [21,74–84], hydrogen-bonding organics [21,74,77,78,81,85], inorganic network glass formers [21,78,81,86–89], ionic glass formers [21,81,90,91], metallic glass formers [92–106], polymeric glass formers [19,21,68,81,107–115], aromatic polymer glasses [108,116–124], ionic liquids [72,125–149] and ambers [73].

Table 2 Slopes of the linear regression lines of Figs. 7(a) and 7(b). characterizing the strength of the T_g-dependences of $m(T_g)$ and $E_a(T_g)$ in different classes of glass-forming liquids. Standard errors are given in parenthesis.

	T_g-dependence of $m(T_g)$ ($m(T_g) \sim a \times T_g$)	T_g-dependence of $E_a(T_g)$ ($E_a(T_g) \sim b \times T_g$)
Bitumens	0.74(±0.04)	4.35(±0.19)
Small-molecule organics	0.08(±0.07)	1.67(±0.22)
Hydrogen-bonding organics	0.25(±0.06)	2.01(±0.25)
Inorganic network glasses	-0.01(±0.006)	0.47(±0.09)
Ionic glasses	-0.01(±0.09)	1.22(±0.43)
Metallic glasses	0.17(±0.02)	3.43(±0.31)
Polymeric glasses	0.28(±0.07)	3.72(±0.43)
Aromatic polymer glasses	0.17(±0.11)	2.08(±0.60)
Ionic liquids	0.40(±0.18)	3.50(±0.73)
Ambers	0.19(±0.28)	3.26(±2.21)

A comparison of the T_d values obtained from the fits of the modified Kaelble equation with the T_g values measured by DSC is presented in Fig. 8. As described in Section 2.2., T_d can be considered as the rheological glass transition temperature. For the investigated bitumen samples, however, T_d values are observed to be systematically higher than calorimetric T_g values. This observation re-emphasizes the fact that the temperature dependence of viscoelastic properties deviates from the WLF/VFT behavior already significantly above T_g, and therefore Eqs. (4) and (5) do not yield reliable values for $m(T_g)$ and $E_a(T_g)$. The difference between the two temperatures is up to 30 K, being largest in the samples that have lowest T_g. Furthermore, the dispersion of T_d values is observed to be smaller than that of T_g values. It therefore appears that T_d itself is not a sensitive parameter to differentiate different types of bitumens in terms of their glass transition properties.

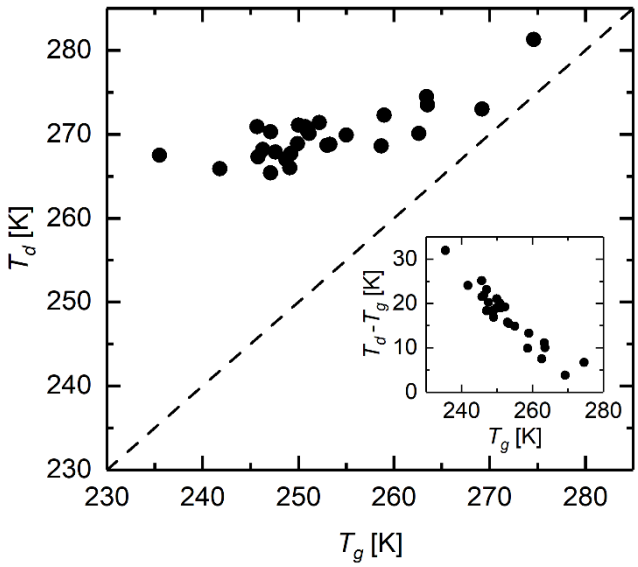

Fig. 8 Comparison of the T_d temperatures obtained from the fits of the modified Kaelble equation and glass transition temperatures (T_g) measured by DSC. The dashed line represents the line of equality ($T_g = T_d$). The inset shows the temperature difference T_d-T_g as a function of T_g.

Because of the difference between T_d and T_g, the dynamic fragility and activation energy values evaluated at these two characteristic temperatures are also significantly different (see Table 1). Somewhat surprisingly, m and E_a values evaluated at T_d (corresponding to the maximum values of these parameters as explained in Section 2.2.) are almost independent of the type of bitumen, $m(T_d) = 57\pm7$ and $E_a(T_d) = 278\pm46$ kJ/mol. The nearly constant values of $m(T_d)$ mean that the viscoelastic properties of the different bitumen samples exhibit almost identical temperature dependence in the vicinity of T_d. This is demonstrated in the modified Angell plot of Fig. 9 where log a_T is plotted against T_d/T. However, although $m(T_d)$ and $E_a(T_d)$ values show only little variation among the investigated bitumen samples, weak positive dependences on T_d can be observed in Fig. 10 (although these dependences are not nearly as strong as the T_g-dependences of $m(T_g)$ and $E_a(T_g)$ reported in Fig. 6).

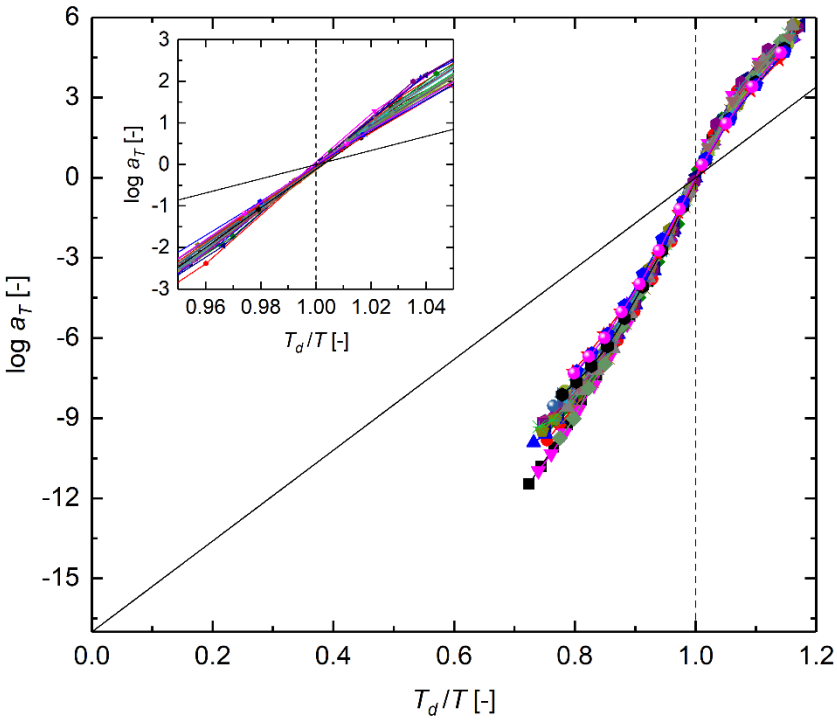

Fig. 9 Modified Angell plot of the investigated bitumen samples. In contrast to the conventional Angell plot, temperatures on the x-axis are normalized with respect to T_d instead of T_g. The inset shows a magnification of the plot in the vicinity of T_d (i.e. $T_d/T \approx 1$). The solid line corresponds to the Arrhenius temperature dependence (m = 17) of a strong glass-forming liquid.

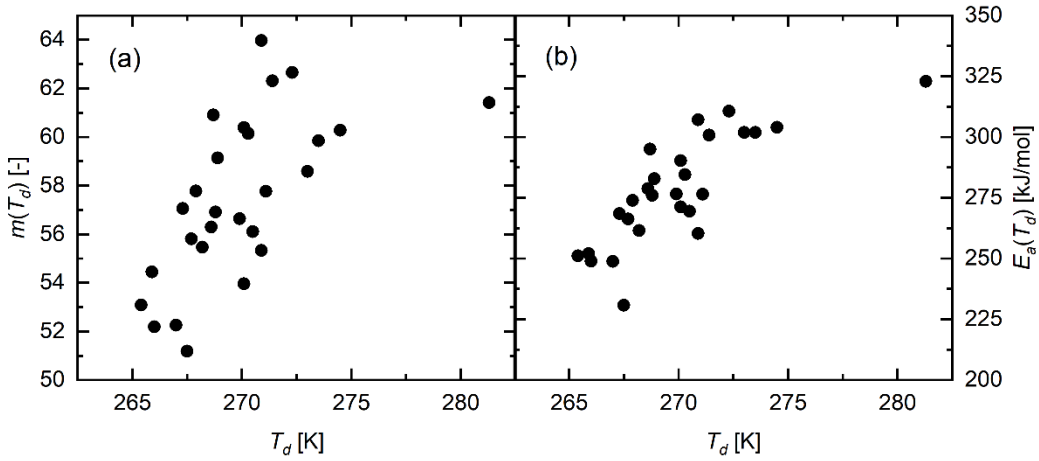

Fig. 10 T_d-dependences of (a) dynamic fragility and (b) apparent activation energy values evaluated at T_d.

It is also of interest to examine the values of the c_1^g and c_2^g parameters of the modified Kaelble equation. It can be seen from Table 1 that the c_1^g values vary in the range of 16.5 to 31.9 (the average value being 20.2), while the c_s^g values vary from 78.7 to 173.6 K (with the average of 102.4 K). Interestingly, a strong positive linear correlation (R^2 = 0.92) is found between these two parameters as shown in Fig. 11. To the best of our knowledge, there are no previous reports of this type of correlation. There is no fundamental reason either why c_1^g and c_2^g should be interrelated. Consequently, the physical meaning of this correlation remains unclear for the time being.

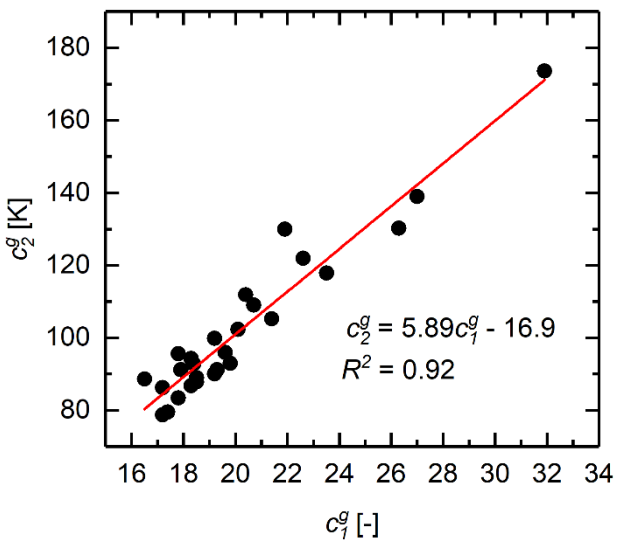

Fig. 11 Correlation between the c_1^g and c_2^g parameters obtained from the fits of the modified Kaelble equation.

5. Conclusions

In this paper, we have derived analytical expressions that allow the calculation of the dynamic fragility and apparent activation energy from the fits of the modified Kaelble equation. As opposed to the WLF and VFT equations, the modified Kaelble equation predicts non-diverging time scales below T_g that are consistent with experimental data. Moreover, the modified Kaelble equation defines the temperature T_d at which an inflection point occurs in the log a_T versus T and log a_T versus T_g/T curves, corresponding to the maximum value of the dynamic fragility and apparent activation energy. The derived analytical solutions are applied to calculate dynamic fragilities and apparent activation energies in twenty-seven bitumens originating from various crude oil sources and refining processes. Bitumen can be considered as a strong glass-forming liquid, dynamic fragility values varying in the range of $m(T_g) = 26 \ldots 52$ for the investigated bitumen samples. Interestingly, different bitumen samples exhibit significant differences in the temperature dependence of their viscoelastic properties only in the close vicinity of T_g. Based on an extensive analysis of literature data, the T_g-dependences of $m(T_g)$ and $E_a(T_g)$ are stronger in bitumen than in any other class of glass-forming liquids. However, the dynamic fragility and apparent activation energy values show much smaller variation among different bitumen samples when evaluated at T_d. Finally, we report an empirical linear correlation between the c_1^g and c_2^g parameters of the modified Kaelble equation. The extension of the present analysis to other types of glass-forming liquids remains as a topic for future research.

Acknowledgment

OVL acknowledges financial support from the Osk. Huttunen Foundation.

References

[1] J. Read, D. Whiteoak, The Shell Bitumen Handbook, 5th ed., Thomas Telford, London, UK, 2003.

[2] D. Lesueur, The colloidal structure of bitumen: Consequences on the rheology and on the mechanisms of bitumen modification, Adv. Colloid Interface Sci. 145 (2009) 42–82. doi:10.1016/j.cis.2008.08.011.

[3] J.F. Branthaver, J.C. Petersen, R.E. Robertson, J.J. Duvall, S.S. Kim, P.M. Harnsberger, T. Mill, E.K. Ensley, F.A. Barbour, J.F. Scharbron, Binder characterization and evaluation. Volume 2: Chemistry, Strategic Highway Research Program, National Research Council, Washington, DC, 1993.

[4] D.R. Jones, SHRP materials reference library: Asphalt cements: A concise data compilation, Strategic Highway Research Program, National Research Council Washington, DC, 1993.

[5] P. Redelius, H. Soenen, Relation between bitumen chemistry and performance, Fuel 140 (2015) 34–43.

[6] H. Soenen, P. Redelius, The effect of aromatic interactions on the elasticity of bituminous binders, Rheol. Acta 53 (2014) 741–754. doi:10.1007/s00397-014-0792-0.

[7] H. Soenen, X. Lu, O.-V. Laukkanen, Oxidation of bitumen: molecular characterization and influence on rheological properties, Rheol. Acta 55 (2016) 315–326.

[8] Q. Qin, J.F. Schabron, R.B. Boysen, M.J. Farrar, Field aging effect on chemistry and rheology of asphalt binders and rheological predictions for field aging, Fuel 121 (2014) 86–94.

[9] J.G. Speight, The chemistry and technology of petroleum, 5th ed., CRC press, Boca Raton, FL, 2014.

[10] O.-V. Laukkanen, H.H. Winter, H. Soenen, J. Seppälä, Systematic broadening of the viscoelastic and calorimetric glass transitions in complex glass-forming liquids, J. Non. Cryst. Solids 483 (2018) 10–17. doi:10.1016/j.jnoncrysol.2017.12.029.

[11] O.-V. Laukkanen, H.H. Winter, H. Soenen, J. Seppälä, An empirical constitutive model for complex glass-forming liquids using bitumen as a model material, Rheol. Acta 57 (2018) 57–70. doi:10.1007/s00397-017-1056-6.

[12] O.-V. Laukkanen, H.H. Winter, H. Soenen, J. Seppälä, Rheological analysis of bitumen as a complex glass-forming liquid and comparison with some simple glass-forming liquids, Annu Trans Nord Rheol Soc 24 (2016) 17–21.

[13] T.F. Turner, J.F. Branthaver, DSC studies of asphalts and asphalts components, Asph. Sci. Technol. (1997) 59–101.

[14] J.M. Jiménez-Mateos, L.C. Quintero, C. Rial, Characterization of petroleum bitumens and their fractions by thermogravimetric analysis and differential scanning calorimetry, Fuel 75 (1996) 1691–1700.

[15] P. Claudy, J.M. Letoffe, G.N. King, J.P. Plancke, Characterization of asphalts cements by thermomicroscopy and differential scanning calorimetry: Correlation to classic physical properties, Fuel Sci. Technol. Int. 10 (1992) 735–765.

[16] P. Claudy, J.-M. Létoffé, G.N. King, J.-P. Planche, Caractérisation des bitumes routiers par analyse calorimétrique différentielle (ACD). Analyse thermo-optique (ATO).

Corrélation entre propriétés physiques et résultats ACD, Bull. Liaison Labo. Ponts Chaussées 177 (1992) 45–51.

[17] R.J. Schmidt, L.E. Santucci, A practical method for determining the glass transition temperature of asphalts and calculation of their low temperature viscosities, Assoc Asph. Paving Technol Proc 35 (1966) 61–90.

[18] Q. Qin, G.B. McKenna, Correlation between dynamic fragility and glass transition temperature for different classes of glass forming liquids, J. Non-Cryst. Solids 352 (2006) 2977. doi:10.1016/j.jnonerysol.2006.04.014.

[19] D.J. Plazek, K.L. Ngai, Correlation of polymer segmental chain dynamics with temperature-dependent time-scale shifts, Macromolecules 24 (1991) 1222–1224. doi:10.1021/ma00005a044.

[20] R. Böhmer, C.A. Angell, Correlations of the nonexponentiality and state dependence of mechanical relaxations with bond connectivity in Ge-As-Se supercooled liquids, Phys. Rev. B 45 (1992) 10091.

[21] R. Böhmer, K.L. Ngai, C.A. Angell, D.J. Plazek, Nonexponential relaxations in strong and fragile glass formers, J. Chem. Phys. 99 (1993) 4201–4209. doi:10.1063/1.466117.

[22] H. Vogel, The law of the relation between the viscosity of liquids and the temperature, Phys. Z 22 (1921) 645–646.

[23] G.S. Fulcher, Analysis of recent measurements of the viscosity of glasses, J. Am. Ceram. Soc. 8 (1925) 339–355. doi:10.1111/j.1151-2916.1925.tb16731.x.

[24] G. Tammann, W. Hesse, Die Abhängigkeit der Viscosität von der Temperatur bie unterkühlten Flüssigkeiten, Zeitschrift Für Anorg. Und Allg. Chemie 156 (1926) 245–257. doi:10.1002/zaac.19261560121.

[25] M.L. Williams, R.F. Landel, J.D. Ferry, The temperature dependence of relaxation mechanisms in amorphous polymers and other glass-forming liquids, J. Am. Chem. Soc. 77 (1955) 3701–3707. doi:10.1021/ja01619a008.

[26] G.B. McKenna, J. Zhao, Accumulating evidence for non-diverging time-scales in glass-forming fluids, J. Non. Cryst. Solids 407 (2015) 3–13. doi:10.1016/j.jnoncrysol.2014.08.012.

[27] J.C. Dyre, N.B. Olsen, T. Christensen, Local elastic expansion model for viscous-flow activation energies of glass-forming molecular liquids, Phys. Rev. B - Condens. Matter Mater. Phys. 53 (1996) 2171–2174. doi:10.1103/PhysRevB.53.2171.

[28] J.C. Mauro, Y. Yue, A.J. Ellison, P.K. Gupta, D.C. Allan, Viscosity of glass-forming liquids, Proc. Natl. Acad. Sci. 106 (2009) 19780–19784. doi:10.1073/pnas.0911705106.

[29] Q. Zheng, J.C. Mauro, Viscosity of glass-forming systems, J. Am. Ceram. Soc. 100 (2017) 6–25. doi:10.1111/jace.14678.

[30] Y.S. Elmatad, D. Chandler, J.P. Garrahan, Corresponding states of structural glass formers, J. Phys. Chem. B 113 (2009) 5563–5567. doi:10.1021/jp810362g.

[31] Y.S. Elmatad, D. Chandler, J.P. Garrahan, Corresponding states of structural glass formers. II, J. Phys. Chem. B 114 (2010) 17113–17119. doi:10.1021/jp1076438.

[32] I. Avramov, A. Milchev, Effect of disorder on diffusion and viscosity in condensed systems, J. Non. Cryst. Solids 104 (1988) 253–260. doi:10.1016/0022-3093(88)90396-1.

[33] E.A. Di Marzio, A.J.M. Yang, Configurational entropy approach to the kinetics of glasses, J. Res. Natl. Inst. Stand. Technol. (1997). doi:10.6028/jres.102.011.

[34] S. Mirigian, K.S. Schweizer, Elastically cooperative activated barrier hopping theory of relaxation in viscous fluids.I.General formulation and application to hard sphere fluids, J. Chem. Phys. (2014). doi:10.1063/1.4874842.

[35] S.A. Hutcheson, G.B. McKenna, The measurement of mechanical properties of glycerol, m -toluidine, and sucrose benzoate under consideration of corrected rheometer compliance: An in-depth study and review, J. Chem. Phys. 129 (2008). doi:10.1063/1.2965528.

[36] X. Shi, A. Mandanici, G.B. McKenna, Shear stress relaxation and physical aging study on simple glass-forming materials, J. Chem. Phys. 123 (2005) 174507. doi:10.1063/1.2085050.

[37] T. Hecksher, A.I. Nielsen, N.B. Olsen, J.C. Dyre, Little evidence for dynamic divergences in ultraviscous molecular liquids, Nat. Phys. 4 (2008) 737–741. doi:10.1038/nphys1033.

[38] P. Badrinarayanan, S.L. Simon, Origin of the divergence of the timescales for volume and enthalpy recovery, Polymer (Guildf). 48 (2007) 1464–1470. doi:10.1016/j.polymer.2007.01.064.

[39] S.L. Simon, J.W. Sobieski, D.J. Plazek, Volume and enthalpy recovery of polystyrene, Polymer (Guildf). 42 (2001) 2555–2567. doi:10.1016/S0032-3861(00)00623-6.

[40] J. Zhao, G.B. McKenna, Temperature divergence of the dynamics of a poly(vinyl acetate) glass: Dielectric vs. mechanical behaviors, J. Chem. Phys. 136 (2012). doi:10.1063/1.3701736.

[41] P.A. O'Connell, G.B. McKenna, Arrhenius-type temperature dependence of the segmental relaxation below Tg, J. Chem. Phys. 110 (1999) 11054–11060. doi:10.1063/1.479046.

[42] J. Zhao, S.L. Simon, G.B. McKenna, Using 20-million-year-old amber to test the super-Arrhenius behaviour of glass-forming systems, Nat. Commun. 4 (2013). doi:10.1038/ncomms2809.

[43] R. Nozaki, S. Mashimo, Dielectric relaxation measurements of poly(vinyl acetate) in glassy state in the frequency range 10−6–106 Hz, J. Chem. Phys. 87 (1987) 2271. doi:10.1063/1.453156.

[44] C.M. Clarkson, J.D. McCoy, J.M. Kropka, Enthalpy recovery and its relation to shear response in an amine cured DGEBA epoxy, Polym. (United Kingdom) 94 (2016) 19–30. doi:10.1016/j.polymer.2016.03.095.

[45] M.L. Cerrada, G.B. McKenna, Physical aging of amorphous PEN: Isothermal, isochronal and isostructural results, Macromolecules 33 (2000) 3065–3076. doi:10.1021/ma990400a.

[46] P. Shi, R. Schach, E. Munch, H. Montes, F. Lequeux, Glass transition distribution in miscible polymer blends: from calorimetry to rheology, Macromolecules 46 (2013) 3611–3620.

[47] K.C. Rusch, R.H.B. Jr, Yielding behavior of glassy polymers. III. Relative influences of free volume and kinetic energy, J. Macromol. Sci. Part B Phys. 4 (1970) 621–633. doi:10.1080/00222347008229378.

[48] K.C. Rusch, R.H. Beck, Yielding behavior of glassy polymers. I. Free-volume model, J. Macromol. Sci. Part B 3 (1969) 365–383. doi:10.1080/00222346908217099.

[49] K.C. Rusch, Time-temperature superposition and relaxational behavior in polymeric glasses, J. Macromol. Sci. Part B Phys. 2 (1968) 179–204. doi:10.1080/00222346808212448.

[50] D.H. Kaelble, Physical chemistry of adhesion, Wiley-Interscience, New York, NY, 1971.

[51] J.S. Vrentas, J.L. Duda, A free-volume interpretation of the influence of the glass transition on diffusion in amorphous polymers, J. Appl. Polym. Sci. 22 (1978) 2325–2339. doi:10.1002/app.1978.070220823.

[52] B. Meissner, Generalization of the WLF equation and of the free-volume concept for the description of transport phenomena in the glassy region, J. Polym. Sci. Part C Polym. Lett. 19 (1981) 137–142. doi:10.1002/pol.1981.130190309.

[53] B. Fan, D.O. Kazmer, Low-temperature modeling of the time-temperature shift factor for polycarbonate, Adv. Polym. Technol. 24 (2005) 278–287. doi:10.1002/adv.20049.

[54] D.H. Kaelble, Computer Aided Design of Polymers and Composites, Marcel Dekker, New York, NY, pp. 145-147, 1985.

[55] G.M. Rowe, M.J. Sharrock, Alternate shift factor relationship for describing temperature dependency of viscoelastic behavior of asphalt materials, Transp. Res. Rec. J. Transp. Res. Board 2207 (2011) 125–135. doi:10.3141/2207-16.

[56] G. Rowe, G. Baumgardner, M. Sharrock, Functional forms for master curve analysis of bituminous materials, in: A. Loizos, M.N. Partl, T. Scarpas, I.L. Al-Qadi (Eds.), Proceedings of the 7th international RILEM symposium ATCBM09 on advanced testing and characterization of bituminous materials, Taylor & Francis Ltd, London, UK, 2016: pp. 81–91.

[57] O.-V. Laukkanen, H.H. Winter, H. Soenen, Rheological analysis of the low-temperature dynamics of bitumens, Annu. Trans. Nord. Rheol. Soc. 23 (2015) 23–26.

[58] N.I.M. Yusoff, E. Chailleux, G.D. Airey, A comparative study of the influence of shift factor equations on master curve construction, Int. J. Pavement Res. Technol. 4 (2011) 324–336. doi:10.6135/ijprt.org.tw/2011.4(6).324.

[59] A. Arikoglu, A new fractional derivative model for linearly viscoelastic materials and parameter identification via genetic algorithms, Rheol. Acta 53 (2014) 219–233. doi:10.1007/s00397-014-0758-2.

[60] J. Rieger, The glass transition temperature Tg of polymers—comparison of the values from differential thermal analysis (DTA, DSC) and dynamic mechanical measurements (torsion pendulum), Polym. Test. 20 (2001) 199–204.

[61] R. Christensen, Theory of viscoelasticity: an introduction, 2nd ed., Academic Press, New York, NY, 1982.

[62] O.-V. Laukkanen, Low-temperature rheology of bitumen and its relationship with chemical and thermal properties, M.Sc. thesis, Aalto University, 2015.

[63] C.-Y. Liu, M. Yao, R.G. Garritano, A.J. Franck, C. Bailly, Instrument compliance effects revisited: linear viscoelastic measurements, Rheol. Acta 50 (2011) 537–546.

[64] O.-V. Laukkanen, Small-diameter parallel plate rheometry: a simple technique for

measuring rheological properties of glass-forming liquids in shear, Rheol. Acta 56 (2017) 661–671. doi:10.1007/s00397-017-1020-5.

[65] K. Schröter, S.A. Hutcheson, X. Shi, A. Mandanici, G.B. McKenna, Dynamic shear modulus of glycerol: Corrections due to instrument compliance, J. Chem. Phys. 125 (2006) 214507. doi:10.1063/1.2400862.

[66] O.-V. Laukkanen, H.H. Winter, J. Seppälä, Characterization of physical aging by time-resolved rheometry: Fundamentals and application to bituminous binders. Submitted to Rheologica Acta, (n.d.) Under review.

[67] H. Booij, J. Palmen, Linear viscoelastic properties of melts of miscible blends of poly (methylmethacrylate) with poly (ethylene oxide), in: P. Moldenaers, R. Keunings (Eds.), Theor. Appl. Rheol., Elsevier, Brussels, 1992: pp. 321–323.

[68] K.L. Ngai, C.M. Roland, Intermolecular Cooperativity and the Temperature Dependence of Segmental Relaxation in Semicrystalline Polymers, Macromolecules 26 (1993) 2688–2690. doi:10.1021/ma00063a008.

[69] C.A. Angell, Strong and Fragile Liquids, Relax. Complex Syst. Ed. by K. L. Ngai G. B. Wright (NTIS, Springfield, Va.) (1985) 1–14.

[70] V.W. Oldekop, Theoretische betrachtungen über die Zähigkeit von Gläsern, Glas. Berichte 30 (1957) 8–14.

[71] W.T. Laughlin, WT Laughlin and DR Uhlmann, J. Phys. Chem. 76, 2317 (1972)., J. Phys. Chem. 76 (1972) 2317.

[72] R. Tao, E. Gurung, M.M. Cetin, M.F. Mayer, E.L. Quitevis, S.L. Simon, Fragility of ionic liquids measured by Flash differential scanning calorimetry, Thermochim. Acta 654 (2017) 121–129. doi:10.1016/j.tca.2017.05.008.

[73] J. Zhao, G.B. McKenna, The apparent activation energy and dynamic fragility of ancient ambers, Polym. (United Kingdom) 55 (2014) 2246–2253. doi:10.1016/j.polymer.2014.03.004.

[74] R. Richert, K. Duvvuri, L.T. Duong, Dynamics of glass-forming liquids. VII. Dielectric relaxation of supercooled tris-naphthylbenzene, squalane, and decahydroisoquinoline, J. Chem. Phys. 118 (2003) 1828–1836. doi:10.1063/1.1531587.

[75] R. Casalini, M. Paluch, C.M. Roland, Influence of molecular structure on the dynamics of supercooled van der Waals liquids, Phys. Rev. E 67 (2003) 031505. doi:10.1103/PhysRevE.67.031505.

[76] K. Duvvuri, R. Richert, Dynamics of glass-forming liquids. VI. Dielectric relaxation study of neat decahydro-naphthalene, J. Chem. Phys. 117 (2002) 4414–4418. doi:10.1063/1.1497158.

[77] J.L. Green, K. Ito, K. Xu, C.A. Angell, Fragility in Liquids and Polymers: New, Simple Quantifications and Interpretations, J. Phys. Chem. B 103 (1999) 3991–3996. doi:10.1021/jp983927i.

[78] G. Ruocco, F. Sciortino, F. Zamponi, C. De Michele, T. Scopigno, Landscapes and fragilities, J. Chem. Phys. 120 (2004) 10666–10680. doi:10.1063/1.1736628.

[79] C.M. Roland, M. Paluch, S.J. Rzoska, Departures from the correlation of time- and temperature-dependences of the α-relaxation in molecular glass-formers, J. Chem. Phys. 119 (2003) 12439–12441. doi:10.1063/1.1627295.

[80] S. Hensel-Bielowka, J. Ziolo, M. Paluch, C.M. Roland, The effect of pressure on the structural and secondary relaxations in 1, 1′-bis (p-methoxyphenyl) cyclohexane, J. Chem. Phys. 117 (2002) 2317–2323. doi:10.1063/1.1488593.

[81] D. Huang, G.B. McKenna, New insights into the fragility dilemma in liquids, J. Chem. Phys. 114 (2001) 5621–5630. doi:10.1063/1.1348029.

[82] A. Mandanici, X. Shi, G.B. McKenna, M. Cutroni, Slow dynamics of supercooled m-toluidine investigated by mechanical spectroscopy, J. Chem. Phys. 122 (2005) 114501. doi:10.1063/1.1856919.

[83] R. Casalini, C.M. Roland, Thermodynamical scaling of the glass transition dynamics 1, Phys. Rev. E 062501 (2004) 1–3. doi:10.1103/PhysRevE.69.062501.

[84] L.M. Wang, R. Richert, Identification of dielectric and structural relaxations in glass-forming secondary amides, J. Chem. Phys. 123 (2005) 54516. doi:10.1063/1.1997135.

[85] R. Richert, C.A. Angell, Dynamics of glass-forming liquids. V. On the link between molecular dynamics and configurational entropy, J. Chem. Phys. 108 (1998) 9016–9026. doi:10.1063/1.476348.

[86] C.M. Roland, P.G. Santangelo, D.J. Plazek, K.M. Bernatz, Creep of selenium near the glass temperature, J. Chem. Phys. 111 (1999) 9337–9342. doi:10.1063/1.479846.

[87] V.N. Novikov, Y. Ding, A.P. Sokolov, Correlation of fragility of supercooled liquids with elastic properties of glasses, Phys. Rev. E - Stat. Nonlinear, Soft Matter Phys. 71 (2005) 61501. doi:10.1103/PhysRevE.71.061501.

[88] A. Sipp, D.R. Neuville, P. Richet, Viscosity, configurational entropy and relaxation kinetics of borosilicate melts, J. Non. Cryst. Solids 211 (1997) 281–293. doi:10.1016/S0022-3093(96)00648-5.

[89] E. Rössler, K.U. Hess, V.N. Novikov, Universal representation of viscosity in glass forming liquids, J. Non. Cryst. Solids 223 (1998) 207–222. doi:10.1016/S0022-3093(97)00365-7.

[90] C.A. Angell, Entropy and fragility in supercooling liquids, J. Res. Natl. Inst. Stand. Technol. 102 (1997) 171. doi:10.6028/jres.102.013.

[91] W. Xu, E.I. Cooper, C.A. Angell, Ionic Liquids: Ion Mobilities, Glass Temperatures, and Fragilities, J. Phys. Chem. B 107 (2003) 6170–6178. doi:10.1021/jp0275894.

[92] G.J. Fan, H.-J. Fecht, E.J. Lavernia, Viscous flow of the Pd 43 Ni 10 Cu 27 P 20 bulk metallic glass-forming liquid, Appl. Phys. Lett. 84 (2004) 487–489. doi:10.1063/1.1644052.

[93] V.H. Hammond, M.D. Houtz, J.M. O'Reilly, Structural relaxation in a bulk metallic glass, J. Non. Cryst. Solids 328 (2003) 254. doi:10.1016/s0022-3093(03)00513-1.

[94] T. Komatsu, Application of Fragility Concept To Metallic-Glass Formers, J. Non. Cryst. Solids 185 (1995) 199–202. doi:10.1016/0022-3093(95)00237-5.

[95] J.M. Borrego, A. Conde, S. Roth, J. Eckert, Glass-forming ability and soft magnetic properties of FeCoSiAlGaPCB amorphous alloys, J. Appl. Phys. 92 (2002) 2073–2078. doi:10.1063/1.1494848.

[96] Z.P. Lu, Y. Li, C.T. Liu, Glass-forming tendency of bulk La–Al–Ni–Cu–(Co) metallic glass-forming liquids, J. Appl. Phys. 93 (2003) 286–290. doi:10.1063/1.1528297.

[97] T.A. Waniuk, R. Busch, A. Masuhr, W.L. Johnson, Equilibrium viscosity of the

Zr41.2Ti13.8Cu12.5Ni10Be22.5bulk metallic glass-forming liquid and viscous flow during relaxation, phase separation, and primary crystallization, Acta Mater. 46 (1998) 5229–5236. doi:10.1016/S1359-6454(98)00242-0.

[98] R. Busch, W. Liu, W.L. Johnson, Thermodynamics and kinetics of the Mg 65 Cu 25 Y 10 bulk metallic glass forming liquid, J. Appl. Phys. 83 (1998) 4134–4141. doi:10.1063/1.367167.

[99] D.N. Perera, Compilation of the fragility parameters for several glass-forming metallic alloys, J. Phys. Condens. Matter 11 (1999) 3807. doi:10.1088/0953-8984/11/19/303.

[100] G.J. Fan, E.J. Lavernia, R.K. Wunderlich, H.J. Fecht, The relationship between kinetic and thermodynamic fragilities in metallic glass-forming liquids, Philos. Mag. 84 (2004) 2471–2484. doi:10.1080/1478430410001693454.

[101] S.C. Glade, W.L. Johnson, Viscous flow of the Cu 47 Ti 34 Zr 11 Ni 8 glass forming alloy, J. Appl. Phys. 87 (2000) 7249–7251. doi:10.1063/1.373411.

[102] S. Mukherjee, H.G. Kang, W.L. Johnson, W.K. Rhim, Noncontact measurement of crystallization behavior, specific volume, and viscosity of bulk glass-forming Zr-Al-Co-(Cu) alloys, Phys. Rev. B - Condens. Matter Mater. Phys. 70 (2004) 1–6. doi:10.1103/PhysRevB.70.174205.

[103] B. Zhang, R.J. Wang, D.Q. Zhao, M.X. Pan, W.H. Wang, Properties of Ce-based bulk metallic glass-forming alloys, Phys. Rev. B - Condens. Matter Mater. Phys. 70 (2004) 1–7. doi:10.1103/PhysRevB.70.224208.

[104] G. Wilde, G.P. Görler, R. Willnecker, H.J. Fecht, Calorimetric, thermomechanical, and rheological characterizations of bulk glass-forming Pd 40 Ni 40 P 20, J. Appl. Phys. 87 (2000) 1141–1152. doi:10.1063/1.371991.

[105] Z.F. Zhao, Z. Zhang, P. Wen, M.X. Pan, D.Q. Zhao, W.H. Wang, W.L. Wang, A highly glass-forming alloy with low glass transition temperature, Appl. Phys. Lett. 82 (2003) 4699–4701. doi:10.1063/1.1588367.

[106] I.-R. Lu, G.P. Görler, R. Willnecker, Specific volume of glass-forming liquid Pd43Cu27Ni10P20 and related thermodynamic aspects of the glass transition, Appl. Phys. Lett. 80 (2002) 4534–4536. doi:10.1063/1.1487922.

[107] V.Y. Kramarenko, T.A. Ezquerra, I. Šics, F.J. Baltá-Calleja, V.P. Privalko, Influence of cross-linking on the segmental dynamics in model polymer networks, J. Chem. Phys. 113 (2000) 447. doi:10.1063/1.481809.

[108] C. Alvarez, N.T. Correia, J.J. Moura Ramos, A.C. Fernandes, Glass transition relaxation and fragility in a side-chain liquid crystalline polymer: A study by TSDC and DSC, Polymer (Guildf). 41 (2000) 2907–2914. doi:10.1016/S0032-3861(99)00445-0.

[109] N.T. Correia, C. Alvarez, J.J. Moura-Ramos, Fragility in side-chain liquid crystalline polymers: The TSDC contribution, Polymer (Guildf). 41 (2000) 8625–8631. doi:10.1016/S0032-3861(00)00248-2.

[110] C.M. Roland, P.G. Santangelo, K.L. Ngai, The application of the energy landscape model to polymers, J. Chem. Phys. 111 (1999) 5593. doi:10.1063/1.479861.

[111] S.L. Simon, D.J. Plazek, J.W. Sobieski, E.T. Mcgregor, Physical aging of a polyetherimide: Volume recovery and its comparison to creep and enthalpy measurements, J. Polym. Sci. Part B Polym. Phys. 35 (1997) 929–936. doi:10.1002/(SICI)1099-0488(19970430)35:6<929::AID-POLB7>3.0.CO;2-C.

[112] N.M. Alves, J.L. Gómez Ribelles, J.F. Mano, Enthalpy relaxation studies in polymethyl methacrylate networks with different crosslinking degrees, Polymer (Guildf). 46 (2005) 491–504. doi:10.1016/j.polymer.2004.11.016.

[113] R. Zorn, G.B. McKenna, L. Willner, D. Richter, Rheological Investigation of Polybutadienes Having Different Microstructures over a Large Temperature Range, Macromolecules 28 (1995) 8552–8562. doi:10.1021/ma00129a014.

[114] M. Paluch, C.M. Roland, J. Gapinski, A. Patkowski, Pressure and temperature dependence of structural relaxation in diglycidylether of bisphenol A, J. Chem. Phys. 118 (2003) 3177. doi:10.1063/1.1538597.

[115] C.M. Roland, R. Casalini, Effect of chemical structure on the isobaric and isochoric fragility in polychlorinated biphenyls, J. Chem. Phys. 122 (2005) 134505. doi:10.1063/1.1863173.

[116] J.J.M. Ramos, J.F. Mano, D. Lacey, G. Nestor, Dipolar relaxations in the glass transition region and in the liquid crystalline phase of two side-chain liquid crystalline polysiloxanes, J. Polym. Sci. Part B Polym. Phys. 34 (1996) 2067–2075. doi:10.1002/(SICI)1099-0488(19960915)34:12<2067::AID-POLB12>3.0.CO;2-#.

[117] J.F. Mano, N.T. Correia, J.J. Moura-Ramos, S.R. Andrews, G. Williams, Dipolar relaxation mechanisms in the vitreous state, in the glass transition region and in the mesophase, of a side chain polysiloxane liquid crystal, Liq. Cryst. 20 (1996) 201–217. doi:10.1080/02678299608031127.

[118] J.F. Mano, J.J. Moura-Ramos, Dielectric behaviour of a side-chain-bearing liquid-crystalline polysiloxane, J. Therm. Anal. 44 (1995) 1037–1046. doi:10.1007/BF02547531.

[119] J.F. Mano, J.J. Moura Ramos, D. Lacey, Multiple and inter-related relaxation mechanisms in the mesophase of side-chain liquid crystalline polysiloxanes: A thermally stimulated currents study, Polymer (Guildf). 37 (1996) 3161–3164. doi:10.1016/0032-3861(96)89420-1.

[120] N.T. Correia, J.J. Moura Ramos, Dipolar Motions and Phase Transitions in a Side-Chain Polysiloxane Liquid Crystal. A Study by Thermally Stimulated Depolarization Currents, J. Polym. Sci. Part B Polym. Phys. 37 (1999) 227–235. doi:10.1002/(SICI)1099-0488(19990201)37:3<227::AID-POLB6>3.0.CO;2-E.

[121] J.F. Mano, N.T. Correia, J.J.M. Ramos, A.C. Fernandes, A thermally stimulated discharge currents study of the molecular motions in two polysiloxane side-chain liquid crystalline polymers, J. Polym. Sci., Part B Polym. Phys. 33 (1995) 269–277. doi:10.1002/polb.1995.090330212.

[122] J.J.M. Ramos, J.F. Mano, Dipolar relaxations in a side-chain polyacrylate liquid crystal. A study by thermally stimulated currents, Thermochim. Acta 285 (1996) 347–359. doi:10.1016/0040-6031(96)02905-X.

[123] J.F. Mano, J.J.M. Ramos, A. Fernandes, G. Williams, The dipolar relaxation behaviour of a liquid-crystalline side-chain polymer as studied by thermally stimulated discharge currents, Polymer (Guildf). 35 (1994) 5170–5178. doi:10.1016/0032-3861(94)90466-9.

[124] J.J. Moura-Ramos, J.F. Mano, D. Coates, The thermally stimulated currents spectrum of side-chain liquid crystalline polymers. A further contribution for the attribution of the different discharges at the molecular level, Mol. Cryst. Liq. Cryst. Sci. Technol. A.Molecular Cryst. Liq. Cryst. 281 (1996) 267–278. doi:10.1080/10587259608042250.

[125] J. Leys, M. Wubbenhorst, C.P. Menon, R. Rajesh, J. Thoen, C. Glorieux, P. Nockemann, B. Thijs, K. Binnemans, S. Longuemart, Temperature dependence of the electrical conductivity of imidazolium ionic liquids, J. Chem. Phys. 128 (2008) 64509. doi:10.1063/1.2827462.

[126] F.M. Gaciño, T. Regueira, L. Lugo, M.J.P. Comuñas, J. Fernández, Influence of Molecular Structure on Densities and Viscosities of Several Ionic Liquids, J. Chem. Eng. Data 56 (2011) 4984–4999. doi:10.1021/je200883w.

[127] S.H. Chung, R. Lopato, S.G. Greenbaum, H. Shirota, E.W. Castner, J.F. Wishart, Nuclear Magnetic Resonance Study of the Dynamics of Imidazolium Ionic Liquids with− CH2Si (CH3) 3 vs− CH2C (CH3) 3 Substituents, J. Phys. Chem. B 111 (2007) 4885–4893. doi:10.1021/jp071755w.

[128] H. Shirota, H. Matsuzaki, S. Ramati, J.F. Wishart, Effects of aromaticity in cations and their functional groups on the low-frequency spectra and physical properties of ionic liquids, J. Phys. Chem. B 119 (2014) 9173–9187. doi:10.1021/jp509412z.

[129] J. Pitawala, A. Matic, A. Martinelli, P. Jacobsson, V. Koch, F. Croce, Thermal properties and ionic conductivity of imidazolium bis (trifluoromethanesulfonyl) imide dicationic ionic liquids, J. Phys. Chem. B 113 (2009) 10607–10610. doi:10.1021/jp904989s.

[130] P.B.P. Serra, Thermal behavior and heat capacity of ionic liquids: benzilimidazolium and alkylimidazolium derivatives, M.Sc. thesis, Universidade do Porto, 2013.

[131] J.C. Thermodynamics, P.B.P. Serra, F.M.S. Ribeiro, M.A.A. Rocha, M. Fulem, L.M.N.B.F. Santos, Phase behavior and heat capacities of the 1-benzyl-3-methylimidazolium ionic liquids, J. Chem. Thermodyn. 100 (2016) 124–130. doi:10.1016/j.jct.2016.04.009.

[132] S. V Dzyuba, R.A. Bartsch, Influence of structural variations in 1-alkyl (aralkyl)-3-methylimidazolium hexafluorophosphates and bis (trifluoromethylsulfonyl) imides on physical properties of the ionic liquids, ChemPhysChem 3 (2002) 161–166. doi:10.1002/1439-7641(20020215)3:2<161::AID-CPHC161>3.0.CO;2-3.

[133] R. Tao, S.L. Simon, Rheology of Imidazolium-Based Ionic Liquids with Aromatic Functionality, J. Phys. Chem. B 119 (2015) 11953–11959. doi:10.1021/acs.jpcb.5b06163.

[134] R. Tao, G. Tamas, L. Xue, S.L. Simon, E.L. Quitevis, Thermophysical properties of imidazolium-based ionic liquids: the effect of aliphatic versus aromatic functionality, J. Chem. Eng. Data 59 (2014) 2717–2724. doi:10.1021/je500185r.

[135] N. V. Pogodina, M. Nowak, J. Läuger, C.O. Klein, M. Wilhelm, C. Friedrich, Molecular dynamics of ionic liquids as probed by rheology, J. Rheol. (N. Y. N. Y). 55 (2011) 241–256. doi:10.1122/1.3528651.

[136] W. Zheng, A. Mohammed, L.G. Hines, D. Xiao, O.J. Martinez, R.A. Bartsch, S.L. Simon, O. Russina, A. Triolo, E.L. Quitevis, Effect of cation symmetry on the morphology and physicochemical properties of imidazolium ionic liquids, J. Phys. Chem. B 115 (2011) 6572–6584. doi:10.1021/jp1115614.

[137] N. Shamim, G.B. McKenna, Glass Dynamics and Anomalous Aging in a Family of Ionic Liquids above the Glass Transition Temperature, J. Phys. Chem. B 114 (2010) 15742–15752. doi:10.1021/jp1044089.

[138] J. Leys, R.N. Rajesh, P.C. Menon, C. Glorieux, S. Longuemart, P. Nockemann, M.

Pellens, K. Binnemans, Influence of the anion on the electrical conductivity and glass formation of 1-butyl-3-methylimidazolium ionic liquids, J. Chem. Phys. 133 (2010) 34503. doi:10.1063/1.3455892.

[139] C. Krause, J.R. Sangoro, C. Iacob, F. Kremer, Charge transport and dipolar relaxations in imidazolium-based ionic liquids, J. Phys. Chem. B 114 (2010) 382–386. doi:10.1021/jp908519u.

[140] G.J. Kabo, A. V Blokhin, Y.U. Paulechka, A.G. Kabo, M.P. Shymanovich, J.W. Magee, Thermodynamic properties of 1-butyl-3-methylimidazolium hexafluorophosphate in the condensed state, J. Chem. Eng. Data 49 (2004) 453–461. doi:10.1021/je034102r.

[141] H.P. Diogo, S.S. Pinto, J.J. Moura Ramos, Slow molecular mobility in the amorphous solid and the metastable liquid states of three 1-alkyl-3-methylimidazolium chlorides, J. Mol. Liq. 178 (2013) 142–148. doi:10.1016/j.molliq.2012.11.027.

[142] O. Yamamuro, T. Yamada, M. Kofu, M. Nakakoshi, M. Nagao, Hierarchical structure and dynamics of an ionic liquid 1-octyl-3-methylimidazolium chloride, J. Chem. Phys. 135 (2011) 54508. doi:054508\n10.1063/1.3622598.

[143] O. Russina, M. Beiner, C. Pappas, M. Russina, V. Arrighi, T. Unruh, C.L. Mullan, C. Hardacre, A. Triolo, Temperature Dependence of the Primary Relaxation in 1-Hexyl-3-methylimidazolium bis{(trifluoromethyl)sulfonyl}imide, J. Phys. Chem. B 113 (2009) 8469–8474. doi:10.1021/jp900142m.

[144] M.C.C. Ribeiro, Low-frequency Raman spectra and fragility of imidazolium ionic liquids, J. Chem. Phys. 133 (2010) 024503. doi:10.1063/1.3462962.

[145] Y. Shimizu, Y. Ohte, Y. Yamamura, K. Saito, T. Atake, Low-temperature heat capacity of room-temperature ionic liquid, 1-hexyl-3-methylimidazolium bis (trifluoromethylsulfonyl) imide, J. Phys. Chem. B 110 (2006) 13970–13975. doi:10.1021/jp0618330.

[146] P. Griffin, A.L. Agapov, A. Kisliuk, X.-G. Sun, S. Dai, V.N. Novikov, A.P. Sokolov, Decoupling charge transport from the structural dynamics in room temperature ionic liquids, J. Chem. Phys. 135 (2011) 114509. doi:10.1063/1.3638269.

[147] P. Sippel, P. Lunkenheimer, S. Krohns, E. Thoms, A. Loidl, Importance of liquid fragility for energy applications of ionic liquids, Sci. Rep. 5 (2015) 13922. doi:10.1038/srep13922.

[148] L. Xue, E. Gurung, G. Tamas, Y.P. Koh, M. Shadeck, S.L. Simon, M. Maroncelli, E.L. Quitevis, Effect of Alkyl Chain Branching on Physicochemical Properties of Imidazolium-Based Ionic Liquids, J. Chem. Eng. Data 61 (2016) 1078–1091. doi:10.1021/acs.jced.5b00658.

[149] M. Kofu, M. Tyagi, Y. Inamura, K. Miyazaki, O. Yamamuro, Quasielastic neutron scattering studies on glass-forming ionic liquids with imidazolium cations, J. Chem. Phys. 143 (2015) 234502. doi:10.1063/1.4937413.